

Investigations of geopolymeric mixtures based on phosphate washing waste

R. Dabbebi^{a,b,*}, S. Baklouti^a, J.L. Barroso de Aguiar^b, F. Pacheco-Torgal^b, B. Samet^a

^a University of Sfax, Laboratory of Industrial Chemistry, Tunisia

^b University of Minho, C-TAC Research Centre, Guimarães 4800-058, Portugal

Received 29 June 2017; accepted 13 August 2018

Abstract

The extraction of the phosphate ore produces a high amount of waste causing serious environmental problems. This waste, termed as phosphate washing waste, was filtered and dried at 105 °C for 24 h to remove the water. The dried waste was milled and then sieved in a 100 µm sieve. The resulting phosphates washing waste (PWW) particles size are below 70 µm. The phosphate washing waste was calcined at 700 °C and 900 °C. Both calcined and uncalcined waste were investigated with X-ray fluorescence (XRF), X-ray powder diffraction (DRX), Fourier transform infrared (FTIR), simultaneous differential thermal and thermogravimetric analyses (DTA-TG) and particle size analysis. This waste was activated with sodium hydroxide (NaOH) and sodium silicate in order to produce geopolymeric materials. The influence of replacing PWW by 15% of metakaolin was also study. The results show that the highest compressive strength is obtained with metakaolin. The results also showed that compressive strength decreased with the increase of NaOH concentration.

© 2018 Sociedade Portuguesa de Materiais (SPM). Published by Elsevier España, S.L.U. All rights reserved.

Keywords: Phosphate washing waste; Sodium hydroxide; Sodium silicate; Geopolymer

1. Introduction

Waste recycling is an important feature in the context of sustainable development and also important to the circular economy. The natural Gafsa phosphate is extracted by CPG (Gafsa Phosphate Company) from sedimentary deposits of marine origin, their geological origin dates from about 50 million years. The most used techniques by CPG to extract the phosphate are washing and flotation to eliminate mineral and organic impurities. Tunisia is an international pioneer in the field of natural phosphate and mineral fertilizers and it is the second country in the world to develop a large percentage of its production of phosphate (nearly 80%). The treatment of phosphate ore consists in removing the sterile matrix like clay, quartz to increase the percentage of P₂O₅ which can reach 37%. The ore was washed with a flocculent. Afterwards, it was sorted according to the particle size. The biggest particles exceeding 2 mm were stored in heaps and the finest particles with a dimension below 70 µm are the



Fig. 1. Tunisian phosphate sludge pond.

phosphate washing waste. This product was placed in a basin with around a dozen hectares [1,2]. This waste is hazardous in nature constituting a potential source of pollution and its storage creates environmental problems related to land pollution. Fig. 1 shows a view of the sludge pond.

According to Van Deventer et al. [3] geopolymers are further subsets of inorganic polymers, where the binding phase is almost exclusively aluminosilicate and very highly coordinated.

* Corresponding author.

E-mail address: rawiabali@gmail.com (R. Dabbebi).

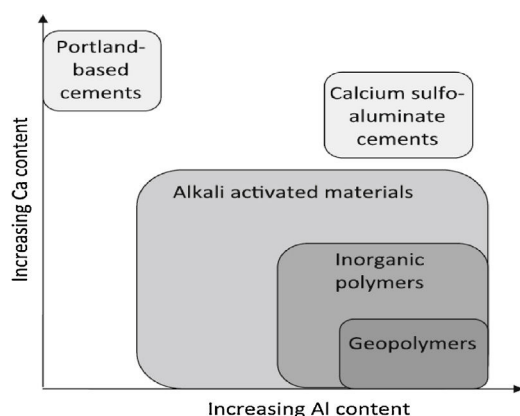


Fig. 2. Classification of different subsets of alkali activated materials with comparisons to OPC and calcium sulfoaluminate binder chemistry.

The available calcium content of the reacting components is usually low; to enable formation of a pseudo-zeolitic network structure rather than the chains characteristic of calcium silicate hydrates.

Fig. 2 shows the distinction between geopolymers and other binders. The activation of aluminosilicates can also be performed with an acid solution such as in the case of phosphate geopolymer or silico phosphate. Geopolymers have the ability to reuse several wastes [4,5]. They still present some shortcomings that need to be addressed such as a high cost and some durability problems [6]. Large number of researchers worked with a variety of raw materials to synthesis geopolymers. However, no work has addressed the use of phosphate washing waste as a raw material. Therefore, this study discloses preliminary results regarding not only the characterization of that raw material but also its geopolymerization.

2. Experimental works

The phosphate washing waste used in this study was taken from Metlawi's storage ponds (laverie VI) a region in the south of Tunisia. The phosphate washing waste was slurry with or without flocculent. Particle size of the slurry with flocculant was characterized by laser diffraction (Fritsch analysette 22 micritec plus). Then, it was filtered and dried at 105 °C for 24 h to remove the water. The dried phosphate washing waste was crushed, and then sieved to 100 μm. It was calcined in a muffle furnace LAB TechDaihan LAB TECH CO.LTD for 2 h with heating rate 5°/min at 700 °C and 900 °C. After calcination the samples were characterized with XRF, XRD and FTIR. The XRF were conducted by X ray fluorescence (Philips X'unique II), the X-ray diffraction (XRD) was conducted on a Bruker D8 Discover with Cu-Kα radiation ($\lambda = 1.54060 \text{ \AA}$) at 40 kV and 40 mA. Each sample was scanned from 5° to 60° at a speed of $0.02^\circ \text{ s}^{-1}$. The FTIR were scanned from 400 to 4000 cm^{-1} wavenumbers using the Fourier Transform infrared model Perkin Elmer spectrum BX spectrometer. The thermal behaviour of the phosphate washing waste was performed under argon atmosphere with heating rate 10 °C/min from ambient to 1000 °C with TA instruments SDT 2960 Simultaneous. The compressive strength

Table 1

Chemical composition (%) of PWW according to calcination temperature.

Oxides	25 °C	700 °C	900 °C
SiO ₂	42	44.3	42.7
Al ₂ O ₃	9.77	10	9.45
CaO	26.5	24.9	26.7
P ₂ O ₅	10	8.49	8.75
Na ₂ O	1.12	1.64	1.50
K ₂ O	0.673	0.798	0.779
MgO	3.09	2.75	2.91
SO ₃	3.39	3.96	4.10
Fe ₂ O ₃	2.31	2.32	2.39
LOI	18	14.7	17

PS: Phosphate sludge.

Moisture of uncalcined PS = 0.1851%.

Melting temperature of PWW T_f °C = 1150 °C.

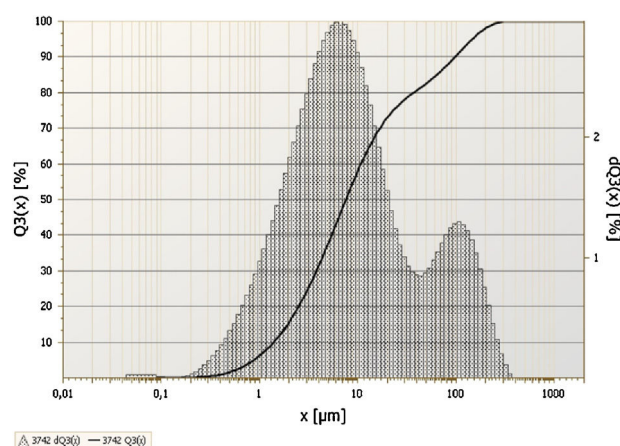


Fig. 3. Particle size analysis of phosphate washing waste with flocculent.

of the consolidate material was evaluated with three cylindrical specimens with 35 mm in diameter and 70 mm in height. The compression tests were carried out using a LLOYD Instruments LR50K apparatus equipped with a 50 kN sensor. The descent rate of the upper platen was set at 0.2 mm/min.

3. Results and discussion

The chemical analysis of phosphate washing waste calcined and uncalcined was done by XRF and the results of this analysis are reported in the Table 1. The table shows that the PWW has an important quantity of SiO₂, CaO, Al₂O₃ and P₂O₅. Figs. 3 and 4 show the distribution of the particles size of the phosphate washing waste with and without flocculent. Fig. 5 shows some samples of phosphate washing waste powder before and after calcination.

With flocculent the distribution is bimodal. The most dominant is between 0.9 and 60 μm, and the majority of particles have a diameter of 7.5 μm. The less dominant population is between 60 and 250 μm, with particles majority having an approximate diameter of 100 μm. The difference of the size particles can be explained by the presence of the flocculent used by the company to recover the maximum of water. Fig. 4 shows the distribution of particles size of the phosphate washing waste without flocculent.

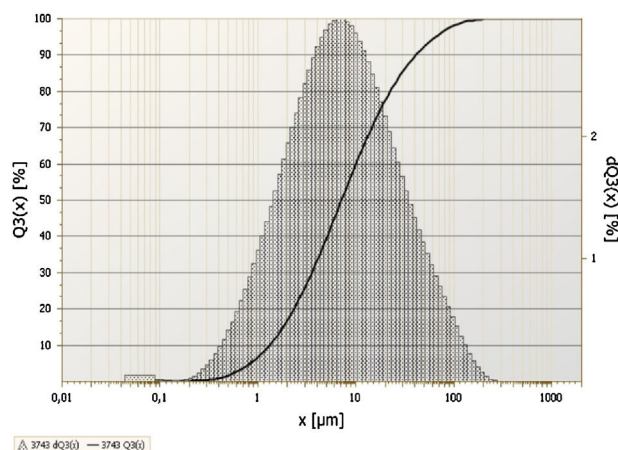


Fig. 4. Particle size analysis of phosphate washing waste without flocculent.

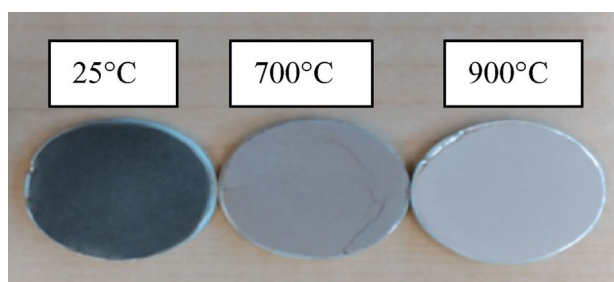


Fig. 5. Phosphate washing waste powder before and after calcinations.

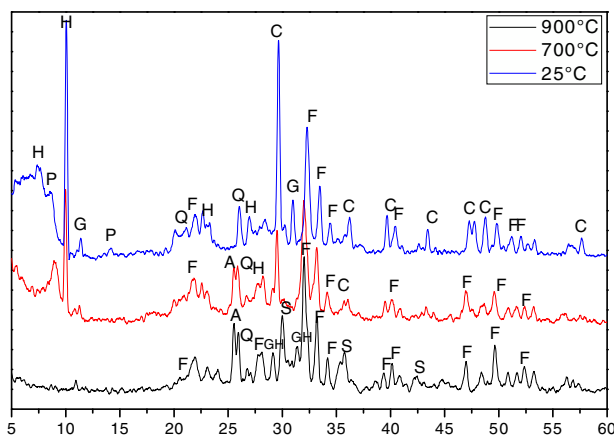


Fig. 6. X ray diffractograms of the phosphate sludge uncalcined and calcined at 700 °C and 900 °C. C: Calcite (PDF: 00-002-0629), H: Heulandites (PDF#01-076-2214), G: Gypsum (PDF#00-021-0816), Q: Quartz (PDF#01-070-2535), F: Fluorapatite (PDF#00-002-0845), P: Palygorskite (PDF#00-029-0855), A: Anhydrite (PDF#00-003-0368), S: Calcium Iron Silicate (PDF#00-003-1134), GH: Gehlenite (PDF#00-001-0982).

The patterns of the XDR show the presence of amorphous and crystalline phases (Fig. 6).

The Ca/P ratio determined by the chemical composition of uncalcined material is $2.65 > 1.67$: this indicates the presence of calcite or dolomite, or that there is a substitution of PO_4 by CO_3 [7], and this was confirmed by the XRD. The diffractogram shows the presence of calcite, fluorapatite, palygorskite, heulandites, quartz and gypsum.

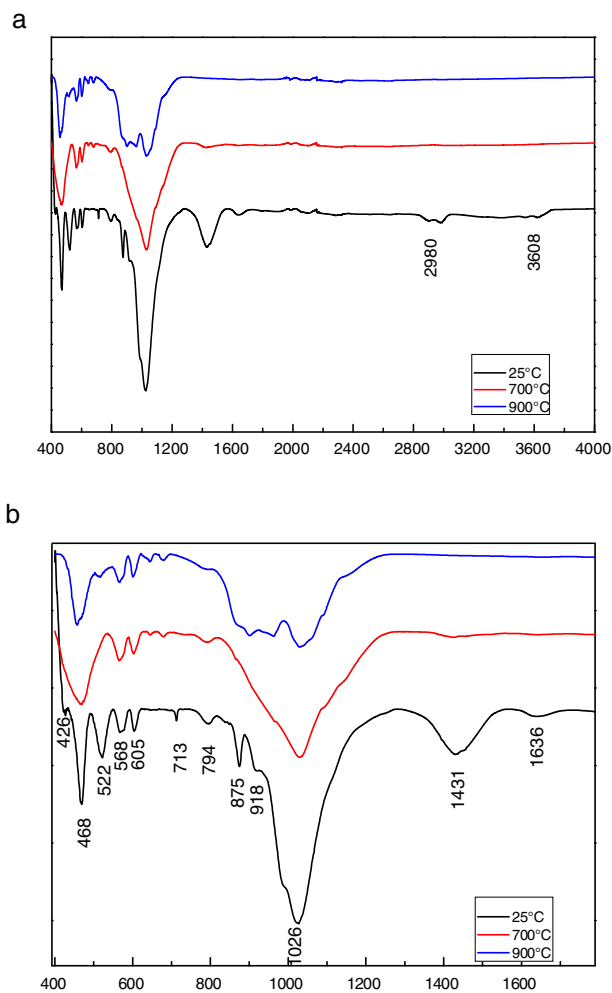


Fig. 7. FTIR spectra of phosphate washing waste. (a) 400–4000 cm^{-1} ; (b) 400–1600 cm^{-1} .

After calcination at 700 °C, the curve shows the disappearance of palygorskite, and the presence of a new phase anhydrite CaSO_4 a decrease in the intensity of the peaks of heulandites and of calcite, this was supported by the FTIR. At 900 °C the curve shows a total disappearance of heulandites and calcite and the appearance of new phase calcium iron silicate and gehlenite.

Fig. 7 shows the FTIR spectra of phosphate washing waste. The examination of the spectral shows bands at 1636–3543 cm^{-1} confirming the presence of the stretching hydroxyl group (OH^-) and these bands disappeared at 700 °C and 900 °C. The peak at 3616 cm^{-1} which characterizes the OH stretching vibration of the palygorskite mineral confirms the results present in the XRD patterns. The organic matter was shown by the presence of band at 2980 cm^{-1} and it disappeared also at 700 °C and 900 °C.

The bands at 713, 875 and 1431 cm^{-1} confirmed the presence of carbonate CO_3^{2-} [8]. These 3 bands were vanished at 900 °C and the weight loss was attributed to the decomposition of carbonates. Asymmetric stretch silicate bands were observed at 1025 cm^{-1} , a deformation band of Si-O-Al at 522 cm^{-1} , a trace of quartz at 794 cm^{-1} and a deformation band at 426 cm^{-1} of Si-O. Two bands at 468 and 568 correspond to PO_4^{3-} . The

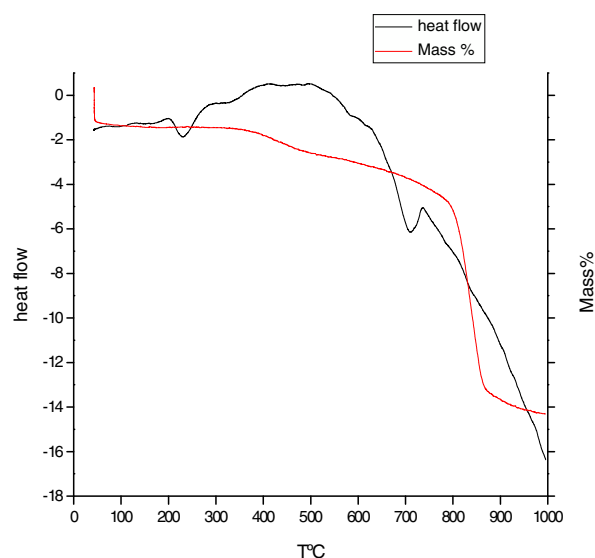


Fig. 8. Thermal behavior of phosphate washing waste.

FTIR spectrum shows also a deformation band at 918 cm^{-1} of Al-OH-Al [9] of the palygorskite.

Fig. 8 shows the thermal behavior of phosphate washing waste, the first mass loss is an endothermic effect around 100°C corresponds to the removal of adsorbed water (moisture). The second mass loss is between 200 and 550°C , an endothermic peak corresponding to structural water of the natural zeolite [10], and an exothermic peak corresponding to the combustion organic matter. The third mass loss is an endothermic peak reflecting the decomposition of carbonates calcite CaCO_3 with release of CO_2 .

Mixtures with phosphate washing waste (uncalcined and calcined at 700°C and 900°C) activated with sodium silicate and sodium hydroxide were tested.

The chemical composition of the sodium silicate solution by mass was Na_2O : 10.6%, SiO_2 : 26.5% and water: 45% with bulk density 1390 kg/m^3 . The sodium hydroxide solution was obtained by dissolving different amount of sodium hydroxide pellets (98% purity) in distilled water to have different concentrations 7, 9, 10, 12 and 14 M before 24 h of the mixing.

The liquid/solid ratio of the mixture was ~ 0.75 . The obtained mixtures were placed in a closed polystyrene mold and compacted with vibrating table to remove entrapped air bubbles. After they were cured at room temperature for 7 days. A summary of the different mixtures is presented in Table 2.

Consolidate material “yes” refers to a solid state after 24 h while non-consolidate material refers to mixtures that were still fresh after 24 h. This are labelled NO in Table 2. S.H refers to NaOH solution. S.S + xM refers to sodium silicate solution with sodium hydroxide solution. Those mixtures were composed by 50% of sodium silicate solution and 50% of sodium hydroxide solution. S.H in S.S refers that the pellets of sodium hydroxide were dissolved in the sodium silicate solution. The uncalcined powder and calcined at 900°C show different results compared with powders calcined at 700°C which implies that the two powders have more stable phases.

Table 2

Summary of the mixtures.

Liquid/solid	N. C.P.S	C.P.S 900 °C	C.P.S 700 °C	C.P.S 700 °C + MK
S.H 7,9,10,12,14 M	NO	NO	NO	NO
S.S	NO	NO	YES	YES
S.H in S.S	NO	NO	NO	NO
S.S + 7 M	NO	NO	YES	YES
S.S + 9 M	NO	NO	YES	YES
S.S + 10 M	NO	NO	YES	YES
S.S + 12 M	NO	NO	YES	YES
S.S + 14 M	NO	NO	YES	YES

N.C.P: uncalcined phosphate sludge; C.P.S: calcined phosphate sludge.

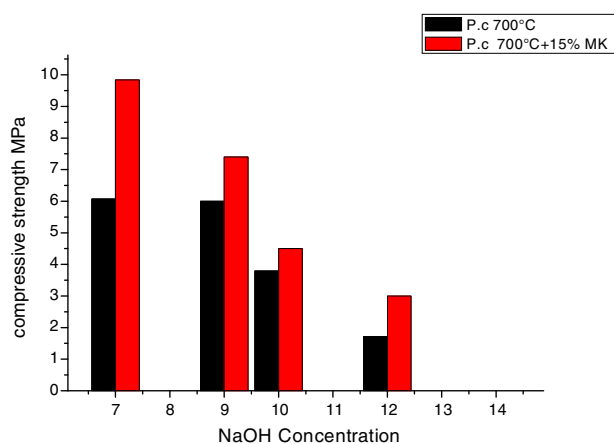


Fig. 9. Compressive strength of the geopolymer with sodium silicate and different NaOH concentration.

Fig. 9 shows the compressive strength results for mixtures with 7 curing days with sodium silicate and sodium hydroxide. The maximum strength (6 MPa) was obtained when using a sodium hydroxide concentration below 10 M. Mixtures show lower compressive strength for higher sodium hydroxide concentration. Mixtures with 15% metakaolin showed a higher compressive strength with a maximum of 10 MPa for a sodium hydroxide concentration of 7 M.

The concentration of sodium hydroxide affects the microstructure and the compressive strength of geopolymers [11]. The increase of NaOH concentration in the aqueous phase of geopolymeric system decreases the dissolution rate of Si and Si-Al phase of phosphate washing waste calcined at 700°C , which affects negatively the mechanical properties of the obtained materials. An excess of hydroxide ion OH^- concentration caused a precipitation of aluminosilicate gel at very early stages, and it will accelerate the dissolution, so the geopolymerisation will be stopped which leads to a lower compressive strength [12]. Moreover, in the condition of high NaOH concentration, the sodium cation consumes the surfaces species (T-OH and T-O-), so the chemical bonding between the insoluble solid particles and geopolymeric framework take place in the final stage of the geopolymerization [13].

Fig. 10 shows the compressive strength results for mixtures with 7 curing days with only sodium silicate as activator.

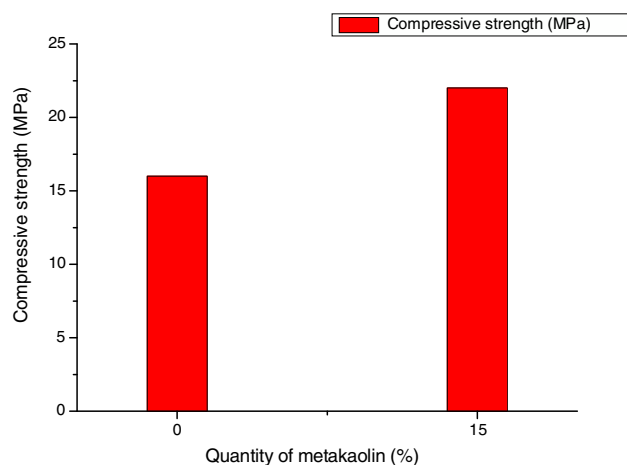


Fig. 10. Compressive strength of the geopolymer with only sodium silicate.

From Fig. 10, the compressive strength of the samples activated with only sodium silicate solution S.S was equal to 16 MPa for the PS. This mixed with 15% of metakaolin shows a compressive equal to 22 MPa. These results were higher compared to the results mentioned in Fig. 9. The results show that the compressive strength depends necessarily on the type of the alkali activators. The results can be explained by the presence of more active silica provided by the sodium silicate which involve in the geopolymerization process and it improves the compressive strength [14]. These types of mixtures were avoided because of the high cost of the sodium silicate [15].

4. Conclusions

In this research, the Tunisian phosphate washing waste was studied by fluorescence X, X-ray diffraction, FTIR, thermal and particle size analysis. The structural changes of phosphate washing waste after calcinations at 700 and 900 °C were studied by fluorescence and X-ray diffraction and FTIR. After the calcination, physical and chemical properties of the phosphate washing waste are affected, and the preliminary tests of geopolymerization confirmed the results. The phosphate sludge can be used as a source material for making geopolymers cured at ambient temperature. The geopolymer pastes and the compressive strength are dependent on the structure of the precursor and on the NaOH concentration. The sodium hydroxide concentration of 7 M with sodium silicate and 15% of metakaolin shows the higher compressive strength after cured 7 days. The results also show that an increase of sodium hydroxide concentration decrease the compressive strength. We should mention also that the compressive strength of geopolymers based on phosphate washing waste and sodium silicate without and with 15% of metakaolin show the higher compressive strength after 7 days of curing: 16 MPa and 22 MPa.

Acknowledgments

The authors acknowledge the Gafsa Phosphate Company “CPG Tunisia” for providing us the phosphate washing waste sample and the Portuguese Foundation for Science and Technology (FCT) for the finance of the project UID/ECI/04047/2013.

References

- [1] K. Boughzela, N. Fattah, K. Bouzouita, H. Ben Hassine, Etude minéralogique et chimique du phosphate naturel d'Oum El Khechab (Gafsa, Tunisie), *Rev. Sci. Matér.* 6 (2015) 11–29.
- [2] M. Loutou, M. Hajjaji, M. Mansori, C. Favotto, R. Hakkou, Phosphate sludge: thermal transformation and use as lightweight aggregate material, *J. Environ. Manag.* 130 (2013) 354–360.
- [3] J. Van Deventer, J. Provis, P. Duxson, D. Brice, Chemical research and climate change as drivers in the commercial adoption of alkali activated materials, *Waste Biomass* 1 (2010) 145–155.
- [4] S. Bernal, E. Rodríguez, A. Kirchheim, J. Provis, Management and valorisation of wastes through use in producing alkali-activated, *J. Chem. Technol. Biotechnol.* 91 (2016) 2365–2388, <http://dx.doi.org/10.1002/jctb.4927>.
- [5] J. Payá, J. Monzó, M. Borrachero, M.M. Tashima, Reuse of aluminosilicate industrial waste materials in the production of alkali-activated concrete binders, in: F. Pacheco-Torgal, J. Labrincha, A. Palomo, C. Leonelli, P. Chindaprasirt (Eds.), *Handbook of Alkali-Activated Cements, Mortars and Concretes*, WoodHead Publishing, Cambridge, 2014, pp. 487–518.
- [6] F. Pacheco-Torgal, Z. Abdollahnejad, S. Miraldo, M. Kheradmand, Alkali-activated cement-based binders (AACB) as durable and cost competitive low CO₂ binders: some shortcomings that need to be addressed, in: J. Sanjayan, A. Nazari (Eds.), *Handbook of Low Carbon Concrete*, Elsevier Science and Tech, Waltham, 2016, pp. 195–216.
- [7] M. Slansky, *Geology of Sedimentary Phosphates*, Elsevier Science Pub. Co. Inc., New York, NY, 1986.
- [8] C.K. Huang, P.F. Kerr, Infrared study of the carbonate minerals, *Am. Mineral.* 45 (3–4) (1960) 311–324.
- [9] S.B. Neji, M. Trabelsi, M.H. Frikha, Activation d'une argile smectite Tunisienne à l'acide sulfurique: rôle catalytique de l'acide adsorbé par l'argile, *J. Soc. Chim. Tunisie* 11 (2009) 191–203.
- [10] J. Gelves, G.S. Gallego, M. Marquez, Mineralogical characterization of zeolites present on basaltic rocks from Combia geological formation, La Pintada (Colombia), *Microporous Mesoporous Mater.* 235 (2016) 9–19.
- [11] K. Somna, C. Jaturapitakkul, P. Kajitvichyanukul, P. Chindaprasirt, NaOH-activated ground fly ash geopolymer cured at ambient temperature, *Fuel* 90 (2011) 2118–2124.
- [12] W. Lee, J. Van Deventer, The effects of inorganic salt contamination on the strength and durability of geopolymers, *Colloids Surf. A: Physicochem. Eng. Aspects* 211 (2002) 115–126.
- [13] D. Parias, I.P. Giannopoulou, T. Perraki, Effect of synthesis parameters on the mechanical properties of fly ash-based geopolymers, *Colloids and Surf. A: Physicochem. Eng. Aspects* 301 (2007) 246–254.
- [14] T. Phoo-ngernkham, S. Hanjitsuwan, N. Damrongwiriyanupap, P. Chindaprasirt, Effect of sodium hydroxide and sodium silicate solutions on strengths of alkali activated high calcium fly ash containing Portland cement, *KSCE J. Civil Eng.* 21 (2016) 2202–2210.
- [15] Z. Abdollahnejad, F. Pacheco-Torgal, T. Félix, W. Tahri, J. Barroso Aguiar, Mix design, properties and cost analysis of fly ash-based geopolymer foam, *Constr. Build. Mater.* 80 (2015) 18–30.